Deglaciation in the tropical Indian Ocean driven by interplay between the regional monsoon and global teleconnections

Rajeev Saraswat [a,*], David W. Lea [b], Rajiv Nigam [a], Andreas Mackensen [c], Dinesh K. Naik [a]

[a] Micropaleontology Laboratory, National Institute of Oceanography, Goa, India
[b] Department of Earth Science, University of California, Santa Barbara, USA
[c] Alfred Wegner Institute for Polar and Marine Research, Bremerhaven, Germany

ARTICLE INFO

ABSTRACT

High resolution climate records of the ice age terminations from monsoon-dominated regions reveal the interplay of regional and global driving forces. Speleothem records from Chinese caves indicate that glacial terminations were interrupted by prominent weak monsoon intervals (WMI), lasting a few thousand years. Deglacial WMIs are interpreted as the result of cold temperature anomalies generated by sea ice feedbacks in the North Atlantic, most prominently during Heinrich Events. Recent modeling results suggest, however, that WMIs reflect changes in the intensity of the Indian rather than the East Asian monsoon. Here we use foraminiferal trace element (Mg/Ca and Ba/Ca) and stable isotope records from a sediment core off the Malabar coast in the southeastern Arabian Sea with centennial-scale resolution to test this hypothesis and to constrain the nature and timing of deglacial climate change in the tropical Indian Ocean. The Malabar deglacial SST record is unique in character and different from other tropical climate records. SST at the Last Glacial Maximum was $2.7 \pm 0.5\,^{\circ}\text{C}$ colder than pre-industrial SST. Deglacial warming started at 18.6 (95% CI range 18.8–18.1) kyr BP, within error of the onset of warming at other tropical sites as well as in Antarctica and the Southern Ocean and either coeval with or up to 1 kyr before the atmospheric CO_2 rise. Warming took place in two steps separated by an interval of stable SST between 15.7 (16.2–14.9) and 13.2 (13.9–12.0) kyr BP. The δ^{18}O-water record and the Ba/Ca record, which is a measure of Indian sub-continent riverine runoff, indicate that the last ice age termination was marked by a prominent weak Indian Monsoon interval interrupted by an intense monsoon phase, as seen in speleothem records and predicted by modeling. A strong correspondence between the timing of the Malabar $\delta^{18}O_{sw}$ record and the Hulu Cave monsoon record suggests that deglacial δ^{18}O changes in both localities dominantly reflect compositional changes in precipitation, likely driven by changes in the North Atlantic.

© 2013 Elsevier B.V. All rights reserved.

1. Introduction

Ice-age terminations are an intriguing aspect of Quaternary climate change. Although the interplay between orbital parameters, atmospheric greenhouse gases, high latitude ice-sheets, thermohaline circulation and other internal climate changes have all been identified as potential causal mechanisms (Alley and Clark, 1999), the exact mechanism of Ice-age terminations is still debated (Denton et al., 2010). Tropical changes in response to rising northern hemisphere insolation and/or rising greenhouse gases have been identified as a potential factor driving deglaciation (Rodgers et al., 2003; Ivanochko et al., 2005; Chiang, 2009; Köhler et al., 2010). Tropical regions can warm polar regions through atmospheric teleconnections (Ding et al., 2011), and sea

ice extent in the polar regions is also influenced by the tropics, especially tropical Indian Ocean temperature and monsoon (Yuan and Martinson, 2000). Paleotemperature records show that deglacial warming in both the tropical Pacific and the Atlantic Ocean proceeded more rapidly than the bulk of global ice-volume change, suggesting an important role played by the tropical regions in deglaciation. A concrete lead-lag relationship has not yet been established for the tropical Indian Ocean.

Tropical regions are also the locale for intense monsoon systems, an integral component of deglacial climate changes. Based on stable oxygen isotopic records of stalagmites from Chinese caves, it has been inferred that glacial terminations were marked by a prominent weak monsoon interval (WMI) which was interrupted by a short-lived phase of strengthened monsoon, the Bølling–Allerød (BA), during termination I (Cheng et al., 2009; Denton et al., 2010). The deglacial WMI is interpreted as the result of cold anomalies generated by sea ice feedbacks in the North Atlantic. However, past monsoon records from the tropical Indian

* Corresponding author. Tel.: +91 832 245 0622; fax: +91 832 245 0603.
E-mail address: rsaraswat@nio.org (R. Saraswat).

Ocean have not been viewed in this perspective. Tropical monsoon changes also contribute to deglaciation by modulating atmospheric methane concentration (Loulerge et al., 2008). The availability of high resolution continuous record of sea-surface temperature (SST) and salinity (SSS) changes covering the last glacial–interglacial transition in the tropical Indian Ocean would aid in evaluating these hypotheses.

Available deglacial SST and SSS records from the northern Indian Ocean have relatively coarse temporal resolution (Saraswat et al., 2005; Dahl and Oppo, 2006; Anand et al., 2008; Saher et al., 2009, Govil and Naidu, 2010; Banakar et al., 2010) or are based on proxies derived from two different biogenic components (alkenone unsaturation ratio and $\delta^{18}O$ planktic foraminifera) (Rostek et al., 1993). Recently, it has been shown that these two proxies may have different habitat preferences such that they incorporate climatic signals from different time periods of the year (Saher et al., 2009). The SST and SSS inferred from the same proxy carrier yields records that cannot be offset in time. Such records can be reconstructed from paired oxygen isotopic ($\delta^{18}O$) and elemental (Mg/Ca—a proxy for past sea surface temperature and Ba/Ca—a proxy for past Indian sub-continent river runoff) analysis of surface dwelling planktic foraminifera recovered from marine sediments (Weldeab et al., 2007; Schmidt and Lynch-Stieglitz, 2011). Here, we present a new high-resolution centennial-scale deglacial history of the tropical Indian Ocean based on elemental and oxygen isotopic analysis of the surface dwelling planktic foraminifera from a core collected from the Lakshadweep Sea, in the southeastern Arabian Sea off the Malabar coast.

2. Materials and methodology

2.1. Core location and oceanographic setting

Core SK237-GC04 (hereafter referred to as the Malabar core) was collected from the continental margin off the Malabar (southwest) coast of India (10°58.65′N, 74°59.96′E) from a water depth of 1245 m (Fig. 1). The core site is located in the eastern part of the Lakshadweep Sea, an area of the Arabian Sea that experiences a distinct annual temperature cycle marked by the development of a mini warm pool with SST peaking at >31 °C in April–May followed by a cooling to <27 °C in August–September associated with coastal upwelling during the later part of the SW monsoon

season (Shankar et al., 2004). During the summer monsoon season, intense northeast winds result in a southward flowing summer monsoon current (Shankar et al., 2002). Conversely, the surface water flow direction reverses during the winter monsoon season, when the winter monsoon current transports 6 Sv of the low salinity Bay of Bengal water into the southeastern Arabian Sea (Shankar et al., 2002). The volume of freshwater influx from the rivers originating in the Western Ghats increases during the southwest monsoon season, resulting in the development of low salinity surface waters off the west coast of India.

2.2. Foraminiferal isotopic and elemental analysis

The Mg/Ca, Ba/Ca and stable oxygen isotopic ratio ($\delta^{18}O$) of the surface dwelling white variety of planktic foraminifera Globigerinoides ruber (white) was measured to reconstruct past sea surface temperature and salinity. The shallow water depth ensures good carbonate preservation, as confirmed by visual examination of the foraminifera and by shell weights. The shells are pristine, with translucent wall and occasionally intact spines. For Mg/Ca and Ba/Ca analysis, 40–50 clean specimens of G. ruber from 250–355 μm size range were picked, weighed, crushed and transferred to plastic centrifuge tubes. The specimens were cleaned following the UCSB standard foraminifera cleaning procedure without the DTPA step (Lea et al., 2000, Martin and Lea, 2002). Thoroughly cleaned samples were analyzed by using a Thermo Finnigan Element2 sector field ICP-MS following the isotope dilution/internal standard method (Martin and Lea, 2002).

SST is calculated from the Mg/Ca ratio by using a depth-corrected calibration equation (Dekens et al., 2002):

$$Mg/Ca = 0.38\exp0.09[SST - 0.61(\text{core depth km})] \qquad (1)$$

We use this calibration, which was originally developed for the Atlantic, because no comparable equation exists for the Indian Ocean and because the pre-exponential and exponential constants have been independently verified by sediment trap studies (Anand et al., 2003). The standard error of this equation, when fit to Atlantic and Pacific core-tops, was estimated at ±1.2 °C. Based on Eq. (1), the reconstructed core-top (average of the top 5 intervals) SST is 28.3 ± 0.3 °C (±1SD), which agrees well with modern SST for the region (28.7 °C) (Locarnini et al., 2006) (Fig. 3). This error, and others reported herein, is based on replicate analyses when available or, if not, on the standard deviation of consistency
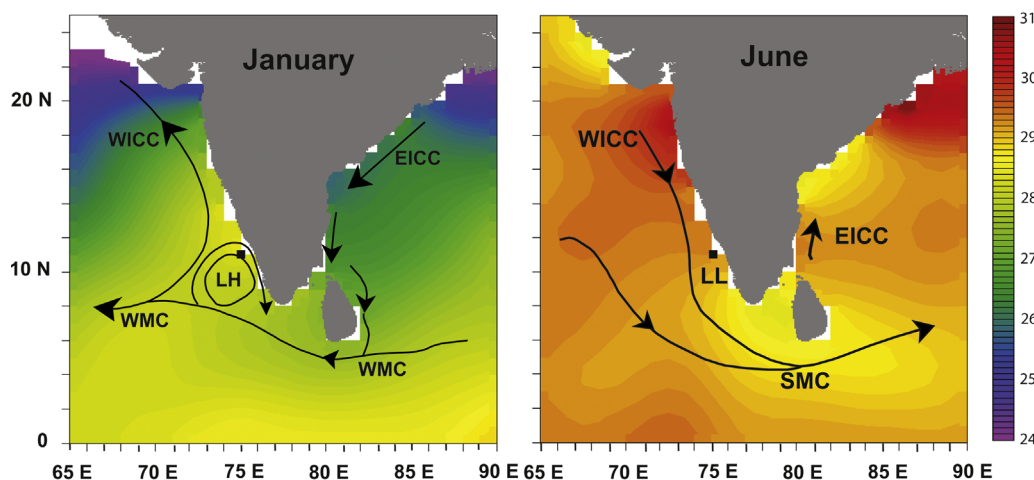

Fig. 1. Seasonal sea surface temperature (Locarnini et al., 2006) and surface currents (Shankar et al., 2002, 2004) in the southeastern Arabian Sea. The January and June SST is shown in color gradient (Locarnini et al., 2006). The black square marks the core location, which lies near the core of warm pool that forms around the Lakshadweep. The current direction reverses during winter and summer monsoon seasons. WMC—Winter Monsoon Current, SMC—Summer Monsoon Current, EICC—East India Coastal Current, WICC—West India Coastal Current, LH—Lakshadweep High, LL—Lakshadweep Low. (For interpretation of the references to color in this figure legend, the reader is referred to the web version of this article.)

standards during the sample run. To avoid repetition and ambiguity, we do not include the calibration error, which is not precisely known for the Indian Ocean region, in reporting SSTs in this work.

We picked 15–20 clean specimens of *G. ruber* from 250 to 355 µm size range for stable oxygen isotopic analyses. Stable isotope ratios were measured at the Alfred Wegener Institute for Polar and Marine Research (Bremerhaven) using a Finnigan MAT 251 isotope ratio gas mass spectrometer, coupled to an automatic carbonate preparation device (Kiel IV) and calibrated via NBS 19 to the PDB scale. The values are given in δ-notation versus (Vienna Pee Dee Belemnite) (VPDB). Precision of oxygen isotope measurements based on repeat analyses of a laboratory standard over a 1 yr period was better than 0.08‰. The $\delta^{18}O$ of foraminifera ($\delta^{18}O_{foram}$) is a function of both the seawater $\delta^{18}O$ ($\delta^{18}O_{sw}$) and temperature. The $\delta^{18}O_{sw}$ is calculated from measured $\delta^{18}O_{foram}$ by subtracting the contribution of SST as estimated from foraminiferal Mg/Ca ratio by using the low-light paleotemperature equation derived for *Orbulina universa* (Bemis et al., 1998; Lea et al., 2000). The error in $\delta^{18}O_{sw}$, calculated from the error on the Mg/Ca and $\delta^{18}O$ calibrations as well as the reproducibility of $\delta^{18}O$ and Mg/Ca measurements, is estimated at ± 0.3‰. It should be noted that this error applies to the absolute value of $\delta^{18}O_{sw}$ reconstructions; the relative errors in assessing downcore trends would undoubtedly be smaller.

2.3. Ba/Ca as proxy for Indian sub-continent riverine runoff

Foraminiferal Ba/Ca ratio was recently proposed as a method to estimate changes in riverine runoff during the geological past (Hall and Chan, 2004; Weldeab et al., 2007; Schmidt and Lynch-Stieglitz, 2011). A change in seawater Ba concentration is a direct consequence of changes in continental runoff, because river water is enriched in Ba, as enhanced by desorption of Ba from suspended material in estuaries (Hall and Chan, 2004). The relationship between seawater Ba concentration and its incorporation in foraminiferal calcite has been established in laboratory culture experiments, wherein it was observed that the foraminiferal Ba/Ca ratio vary linearly with seawater Ba concentration (Lea and Spero, 1992, 1994; Hönisch et al., 2011). The uncertainty associated with foraminiferal Ba/Ca measurements based on the average of the standard deviation of consistency standards and replicate analysis is 2.2%. The top 42 cm of the core, corresponding to the last 5.2 kyr (see below), has anomalously high (2–12 µmol/mol)-and presumably overprinted Ba/Ca values. These high values are likely due to enhanced productivity and increased sulfate reduction during the late Holocene (Agnihotri et al., 2003), which would dissolve sedimentary barite ($BaSO_4$) and release Ba into pore waters, ultimately causing Ba precipitation on the shells, a phenomenon that has been observed in other cores (Weldeab et al., 2007).

Additionally, the desorption of barium adsorbed onto clays (formed in freshwater environment during lower sea-level like during the last glacial period, when sea level was lower) under high sea stands during interglacial periods can also alter seawater Ba/Ca ratio especially in the near coastal sites (Schmidt and Lynch-Stieglitz, 2011).

Upwelling of subsurface waters, with Ba concentration different than that in the surface waters, can also influence Ba/Ca ratio of the surface dwelling planktic foraminifera. Such a possible influence of upwelling on the foraminiferal Ba/Ca ratio can be accessed from the depth profile of water column Ba concentration. Seawater Ba data is not available from the direct region of the Malabar core. GEOSECS data is available, however, from stations in the SW Bay of Bengal (St. 446: 12°29′N, 84°29′E), south of Sri Lanka (St. 447: 4°59′N, 79°57′E) and the south central Arabian Sea (St. 418: 6°11′N, 64°25′E) (L. Chan and J. Edmond, MIT, pers. comm., 1987). This data indicate that surface water Ba in the SW Bay of Bengal is elevated (56.9 nmol/kg) relative to the shallow thermocline (41 nmol/kg at 101 m), as expected from riverine runoff. The station south of Sri Lanka shows a slight elevated Ba (45.6 nmol/kg versus 40.4 nmol/kg at 46 m) whereas the station in the south central Arabian Sea shows minimum values (37.95 nmol/kg) at the surface. These data are consistent with a minimal impact of upwelling in the SE Arabian Sea, although it is difficult to be certain without offshore data. If upwelling to the Malabar site came from 200 m, it would be sufficient to elevate surface Ba by 4–15%, using data from St. 447 and 418. These hypothetical increases would make only a small contribution to the observed down-core Ba/Ca changes in the Malabar core.

2.4. Chronology

The chronology for the core is based on 8 Accelerator Mass Spectrometer radiocarbon dates on mixed planktic foraminifera (Table 1) measured at the Center for Applied Isotope Studies, the University of Georgia, USA. The ^{14}C dates were calibrated by using the marine dataset (Marine09, Reimer et al., 2009) and Calib6.0 version (Stuiver and Reimer, 1993), employing a reservoir correction ΔR for the eastern Arabian Sea of 138 ± 68 yr (Southon et al., 2002). The age model utilizes the calibrated dates as tie-points and assumes linear sedimentation between tie-points. One radiocarbon age at 99.5 cm was omitted as an outlier because it showed a minor age reversal. This point specifically was omitted because its inclusion in a Bayesian age model (see below) shifts the chronology unrealistically over the Younger Dryas interval.

To evaluate the errors on the age model we performed a Bayesian analysis of the age model using the program "Bacon" (Blaauw and Christen, 2011) and including all of the radiocarbon dates. The Bacon age model is largely consistent (deviations < 200 yr) with the utilized tie-point model with the exception of

Table 1
Details of AMS ^{14}C dates. One radiocarbon age at 99.5 cm, was omitted as an outlier because it showed a minor age reversal.

Lab no.	Sample depth (cm)	^{14}C age (yr BP)	^{14}C age error (±)	Calib. age-range (1σ) (yr, BP)	Calib. age-range (2σ) (yr, BP)	Calib. age (median probability) (yr, BP)
UGAMS5378	0.5	620	25	0–146	0–246	115
UGAMS5739	25.5	2730	30	2163–2336	2075–2460	2260
UGAMS5740	49.5	6360	30	6580–6760	6484–6846	6670
UGAMS5935	85.5	9930	30	10,556–10,749	10,506–10,940	10 670
UGAMS5741	99.5	9890	30	10,529–10,688	10,478–10,887	10 620
UGAMS5936	144.5	12 930	30	14,134–14,623	14,066–14,957	14 440
UGAMS5937	156.5	13 860	40	16,142–16,697	15,830–16,806	16 390
UGAMS7195	188.5	15 820	40	18,508–18,668	18,468–18,730	18 573
UGAMS5938	286.5	28 090	80	31,431–31,717	31,353–31,990	31 600

the interval between 11.05 and 13.35 kyr BP, during which the Bacon age model is up to 640 yr younger. This results from the inclusion of the afore-mentioned reversed age at 99.5 cm. Within this interval, between 91 and 108 cm (11.1–12.1 kyr), the tie-point model falls just outside the upper 95% confidence interval of the Bayesian model. We opted to retain the tie-point age model, however, because it produces a more realistic chronology over the Younger Dryas interval (see below). We utilize the 95% confidence intervals of the Bacon age model to provide conservative limits of our age model when discussing specific events (see below). These confidence limits are given in parentheses immediately following a given age throughout the paper.

The Malabar core spans the last ~32 kyr BP, and the core top shows essentially modern conditions (age 120 (95% CI range −290 to 260) yr BP). The sedimentation rate, as inferred from the calibrated AMS ^{14}C dates, averages 9.1 cm kyr and varies from 5.4 cm/kyr between 2.4 and 6.5 kyr to 15.6 cm/kyr between 10.7 and 14.4 kyr; average sample resolution is ~110 yr. The age model indicates that a well-defined deglacial carbon isotope minimum event in the Malabar record occurred between 16.5 (16.8–15.5) and 14.9 (15.4–14.4) kyr BP, with the most negative values occurring between 16.4 (16.7–15.3) and 15.7 (16.2–14.9) kyr BP. The Malabar δ^{13}C minimum is in good agreement with prior dating of the same feature at 15.9 ± 0.2 kyr BP in a low resolution marine core from the eastern equatorial Pacific (Spero and Lea, 2002) and between 16.8 and 14.9 kyr BP in recent high resolution ice core δ^{13}C data (Schmitt et al., 2012); this agreement confirms that the age model is well anchored during the critical deglacial interval.

3. Results and discussion

3.1. A description of the Malabar SST record

The four proxy records (δ^{18}O, Mg/Ca, Ba/Ca, δ^{18}O$_{sw}$) all indicate a clear glacial-to-interglacial pattern largely consistent with prior
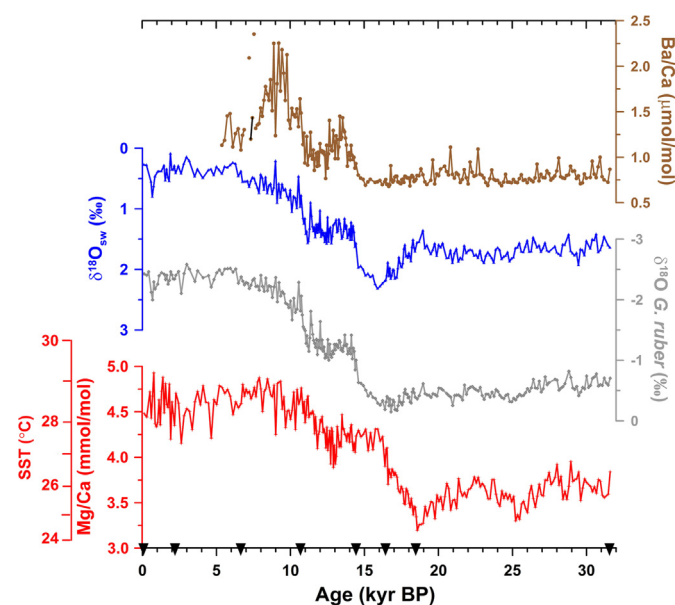

Fig. 2. Variation in *G. ruber* Mg/Ca (SST), Ba/Ca, δ^{18}O and δ^{18}O of seawater in core SK237-GC04 (10°58.65′N, 74°59.96′E, 1247 m water depth). The intervals marking major changes in trace metal and stable isotopic ratio have been dated by AMS radiocarbon and are shown by inverted filled triangles. The average resolution of the data is 110 yr. Ba/Ca data is not shown for the samples younger than 5.4 kyr because the data is likely overprinted by early diagenesis. Two Ba/Ca points are shown as outliers. The onset of deglaciation in Mg/Ca occurs at 18.6 (18.8–18.1) kyr, in δ^{18}O at 16.4 (16.7–15.3) kyr and in Ba/Ca at 15.1 (15.6–14.5) kyr.

high resolution tropical records from monsoon regions (e.g., Weldeab et al., 2007) (Fig. 2). SST estimated from Mg/Ca for the Last Glacial Maximum (LGM) (19–23 kyr, as defined by MARGO) (MARGO Project Members, 2009) indicates that the Lakshadweep Sea was 2.7 ± 0.5 °C colder compared to pre-industrial values, here defined as the average of the top 5 cm of the core, representing the last 500 yr. Peak cooling actually occurred just after the LGM, between 18.6 and 19 (18.1–19.1) kyr, when SST was 3.7 ± 0.4 °C colder than pre-industrial. Previous studies using alkenone unsaturation inferred that the LGM was 1.5–2.5 °C cooler in the northern Indian Ocean (Rostek et al., 1993; Cayre and Bard, 1999). The Mg/Ca-based Malabar record indicates a slightly larger SST change; the observed change is, however, comparable with the 2.8 ± 0.7 °C change recorded for the equatorial Pacific (Lea et al., 2000) and other tropical Indian Ocean records (Saher et al., 2007a; Anand et al., 2008; Govil and Naidu, 2010; Banakar et al., 2010). The 2.7 ± 0.5 °C cooling is also significantly larger than the average annual cooling (1.4 ± 0.7 °C) estimated for the 15°S–15°N tropical band in the Indian Ocean by the MARGO project (MARGO Project Members, 2009). This difference might be due to restricted sample coverage in the Indian Ocean (MARGO Project Members, 2009), proxy differences (Mg/Ca generally yields larger SST changes for the LGM than alkenone unsaturation and faunal abundances), and/or because of better sample resolution (higher sedimentation rate) in the Malabar core.

The Malabar record shows that deglacial warming in the Lakshadweep Sea started at 18.6 (18.8–18.1) kyr BP (Fig. 2). This observation indicates that tropical Indian Ocean warming was synchronous with warming in Antarctica but lead the northern hemisphere warming at the Bølling onset (North Greenland Ice Core Project members, 2004; Jouzel et al., 2007), as also inferred for the tropical Pacific (Lea et al., 2003; Feldberg and Mix, 2003). An initial rapid warming in the Lakshadweep Sea with an increase of 1 °C within ~500 yr was followed by a gradual warming that lasted until 16.6 (17.0–15.6) kyr BP. Another phase of rapid warming (1.3 °C) occurred between 16.6 and 15.7 (16.2–14.9) kyr BP, after which SST stabilized and remained at 27.5 ± 0.5 °C until 13.2 (13.9–12.0) kyr BP. The SST plateau between 15.7 and 13.2 kyr BP is a distinct feature of the Malabar SST record and is discussed in greater detail below. Subsequently, a drop in SST of ~1 °C occurred, centered on 12.9 (13.6−11.7) kyr BP, followed by a stable interval before further warming began at 12.4 (12.7−11.3) kyr BP. Another short cooling phase occurred at 11.8 (11.6−10.9) kyr BP, with a temperature drop of ~1 °C. The early Holocene (centered at 9.7 (10.5−8.7) kyr BP) was also marked by a drop in SST of ~1 °C before the temperature rose to 29 ± 0.1 °C at 9.2 (10.2−8.2) kyr BP. During the Holocene, SST gradually decreased until 2.6 (3.1−2.2) kyr BP, after which SSTs warmed slightly until pre-Industrial times.

The two step deglacial warming observed in the Malabar record is similar to the SST record from the Cariaco basin (Lea et al., 2003) but contrasts with the pattern in the eastern equatorial Atlantic (Weldeab et al., 2007), where a gradual increase in SST is observed during the entire deglaciation. Unlike the Cariaco basin, however, the deglacial Malabar SST record does not show a clear signature of Bølling/Allerød (B/A) warming. The tropical Indian Ocean deglacial SST pattern is unique and does not exactly match the Greenland, Antarctic or other tropical patterns (Fig. 3). This is likely due to the influence of the Indian monsoon on the Malabar SST record, in addition to greenhouse gas and the global albedo forcing. Unlike Antarctic temperature records, which show a distinct warming between 15.7 kyr BP and 14.9 kyr BP, the Malabar SST record is relatively stable during this interval, averaging 27.5 ± 0.3 °C.

The SST record from the Malabar core indicates that prior to the SST minimum within the LGM, two intervals, centered on 22.4
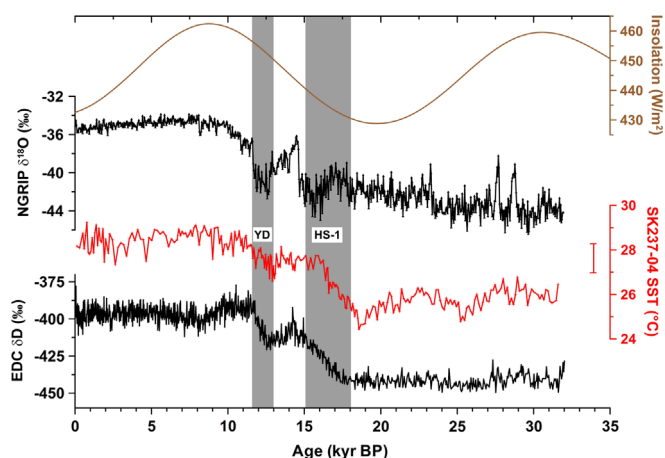
Fig. 3. Comparison of the Malabar SST record with low latitude insolation changes in mid-July at 10°N (Laskar et al., 2004) and the Greenland NGRIP (North Greenland Ice Core Project members, 2004) and Antarctic EDC (Jouzel et al., 2007) proxy temperature records. The red vertical bar shows the overall magnitude of the error associated with Malabar SST. (For interpretation of the references to color in this figure legend, the reader is referred to the web version of this article.)
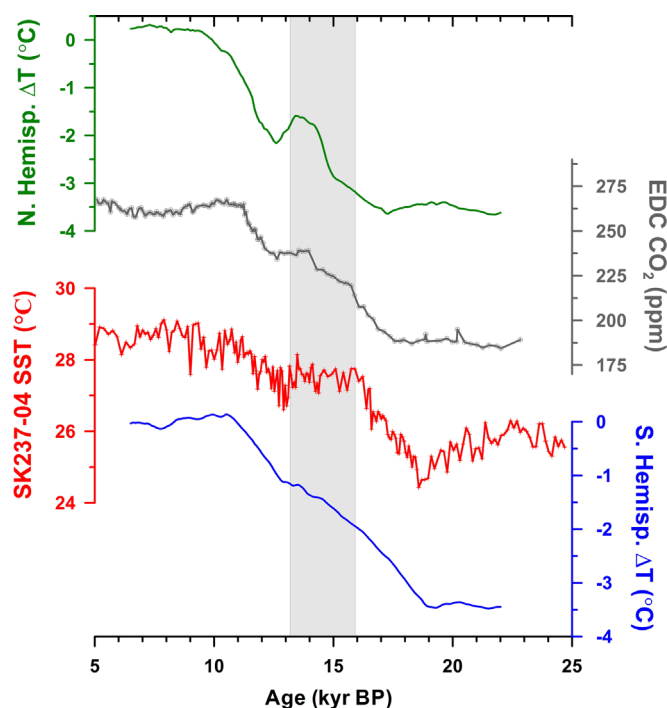
(24.5–20.5) and 28.9 (30.6–26.7) kyr BP, occurred during which SSTs were ∼1–2 °C warmer than during the LGM minimum. The time interval prior to the LGM is also marked by several episodes of rapid rise in SST of ∼1 °C within a couple of centuries (Fig. 3). The character of the Malabar record is more variable during the Holocene, especially after ∼6 kyr BP, with the Mg/Ca data implying several rapid shifts of ∼1 °C.

3.2. Comparison of the Malabar SST record with atmospheric CO_2 rise

One of the biggest enigmas in the relationship between greenhouse gases and global temperatures is the lead of warming over rise in atmospheric CO_2 concentration during the early phase of deglaciation (Monnin et al., 2001). The Malabar record indicates that onset of last deglacial warming in the SE Arabian Sea, at 18.6 (18.8–18.1) kyr BP, might have preceded the increase in atmospheric CO_2 concentration by ∼1 kyr, given that the rise in atmospheric CO_2 concentration as observed in dome C ice records has been dated to 17.6 kyr BP (Lourantou et al., 2010) (Fig. 4). A recent study, however, places the CO_2 rise at ∼18 kyr (Parrenin et al., 2013), in which case the timing of the Malabar SST rise might not be statistically distinguishable from that of the atmospheric CO_2 rise. A similar tropical warming lead over atmospheric CO_2 rise has also been inferred from the Timor Sea region (Sarnthein et al., 2011), as well as a recent global compilation of deglacial warming records (Shakun et al., 2012) (Fig. 4). The SST lead over atmospheric CO_2 is concurrent with the average southern hemispheric warming—but see Parrenin et al. (2013) for a contrasting view. The remainder of the Malabar SST record largely tracks the CO_2 rise, with the exception of the afore-mentioned plateau in SST between 15.7 and 13.2 kyr. The first half of the SST plateau, from 15.7 to 14.0 kyr, coincides with an interval of rising CO_2 and must reflect the offsetting influence of factor(s) other than greenhouse gas forcing. Earlier, a dominant control of atmospheric CO_2 concentration on tropical SST was inferred from low resolution Pacific Ocean records (Lea, 2004), a view largely supported by the Malabar record. The unique and striking aspect of the Malabar record, exemplified by the SST plateau, is the clear interplay it demonstrates between global driving forces such as atmospheric

Fig. 4. Comparison of Termination I warming in the southeastern Arabian Sea (Malabar core) with the average northern and southern hemispheric temperature records (Shakun et al., 2012). The deglacial CO_2 changes in the Antarctic region (Monnin et al., 2001) are plotted to compare the timing of deglacial warming in the tropics and changes in the atmospheric concentration of CO_2. The shaded vertical bar marks the mid-termination SST plateau in the Malabar record, which occurs between 15.7 (16.2–14.9) and 13.2 (13.9–12.0) kyr BP. The minimum that follows the SST plateau, at 12.9 (13.6–11.7) kyr BP, is coeval with similar features in other records and likely occurred during the Younger Dryas stadial.

CO_2 and regional forces such as the Indian monsoon and migration of the ITCZ (see below).

3.3. Factors other than CO_2 that might have driven Malabar SST

Factors other than greenhouse gas forcing undoubtedly influenced Malabar SST over the last 30 kyr BP, explaining the unique character of the record. These influences might have included changes in the Indian Ocean monsoon, low latitude insolation, and teleconnections to the thermohaline circulation. We explore how the latter two mechanisms might have driven deglacial warming below and then consider the influence of the monsoon on rapid changes during the deglaciation in the next section.

A comparison of the Malabar SST record with mid-summer low latitude (10°N) solar insolation (Laskar et al., 2004) indicates that warming of the tropical northern Indian Ocean took place about ∼1 kyr after the rise in low latitude mid-summer insolation (Fig. 3). Changes in eastern equatorial Atlantic SST also correspond to low latitude mid-summer insolation (Weldeab et al., 2007). The relationship in both cores, however, might be biased by a warm water habitat preference of G. ruber. In addition, any argument for summer insolation control on tropical SSTs requires a rectification process, because winter insolation follows the equal and opposite trend.

A suitable mechanism that could link low latitude summer insolation and early deglacial warming in the tropics remains unexplored. At present, tropical SST responds to seasonal insolation changes and wind strength, which also affects ocean–atmosphere heat exchange and therefore SST (McCreary Jr. et al., 1993; Murtugudde and Busalacchi, 1999; Sengupta et al., 2002; Trenberth et al., 2010). The large scale upwelling along the western and south-eastern Arabian Sea, associated with the summer monsoon, also significantly cools the surface waters (Swallow,

1984; McCreary Jr. and Kundu, 1989). The Malabar core lies near the core of the Arabian Sea mini warm pool (ASMWP), which forms a part of the larger tropical Indo-Pacific warm pool (IPWP) (Vinayachandran and Shetye, 1991). The genesis of ASMWP is the result of Rossby wave radiation by coastal Kelvin waves transported from the Bay of Bengal to the south-eastern Arabian Sea. It results in formation of a sea level high of low saline water brought from the Bay of Bengal (Rao and Sivakumar, 1999; Shenoi et al., 1999; Sengupta et al., 2008). Model test results show that currents transporting low saline water to this region are strong even in the absence of summer monsoon winds over the Arabian Sea, but transport requires strong winds over the Bay of Bengal (McCreary Jr. et al., 1993; Shenoi et al., 1999). The low saline water extends down to 60 m followed by a steep increase in salinity leading to a prominent halocline and stable stratification, which could be very sensitive to seasonal insolation changes. The dissipation of the ASMWP is associated with an increase in salinity in the Lakshadweep Sea region, thus weakening the stratification (Shenoi et al., 2005; Nyadjro et al., 2012). Turbulent mixing and upwelling of cold water along the coastal south-eastern Arabian Sea as a result of summer monsoon winds leads to decrease in aerial extent and intensity of Indian Ocean warm pool (Vinayachandran and Shetye, 1991; Shenoi et al., 1999; Neema et al., 2011). A quasi-biweekly mode (QBM), whereby insolation-induced warming of the tropical Indian Ocean during boreal summer is interrupted by the cloud cover generated by the moist convection over the warm ocean, also affects SST in this region. The cloud cover cuts down the insolation, thus cooling the surface waters (Krishnamurti and Bhalme, 1976), a prominent phenomena in both the western Pacific warm pool and the tropical Indian Ocean region during the boreal summer (Chatterjee and Goswami, 2004).

A set of conditions that might have lead to sustained increase in SST in response to rising summer insolation in this region: (1) increased transport of low saline water from the Bay of Bengal to the Malabar region, which would provide a well stratified surface layer sensitive to summer insolation; (2) less availability of moisture source over this region, which would prevent the quasi-biweekly mode of surface cooling; (3) less transport of high saline water by the equator-ward coastal currents along the west coast of India; and (4) the absence of/weaker upwelling, which would prevent early dissipation of the warm pool. The winter monsoon was strong during the glacial interval (Duplessy, 1982; Chodankar et al., 2005; Saher et al., 2007b) with extensive intensification during the early deglaciation (19–17 kyr BP) (Tiwari et al., 2005), leading to high fresh water input into the Bay of Bengal during the last glacial maximum (Rashid et al., 2011). The strong winter winds might have helped increase transport of low saline water from the Bay of Bengal to the south-eastern Arabian Sea (Sarkar et al., 1990), thus fulfilling the first condition. A more southerly position of the ITCZ during the glacial period (Chiang et al., 2003; Broccoli et al., 2006; Gagan et al., 2011) would have contributed to reduced availability of moisture and thus a decrease in cloud formation over this region, as observed during the pre-monsoon season (April), wherein all conditions over this region are conducive for onset of monsoon except the southerly position of ITCZ (Shenoi et al., 1999). It would have significantly reduced cooling associated with QBM. The summer monsoon was weaker during the glacial period (Prell and Kutzbach, 1987; Chodankar et al., 2005; Govil and Naidu, 2010), which would mean weaker equator-ward coastal currents along the west coast of India and absence of or weaker upwelling (Prell, 1984; Naidu and Malmgren, 1996), thus sustaining the summer insolation induced warming for a longer time, as observed in a model run (McCreary Jr. et al., 1993). Such a possibility is further supported by a study which suggests that Indian Ocean part of the IPWP was warmer than the Pacific Ocean region during glacial intervals (Saraswat et al., 2007). Thus we suggest that a link between SE

Arabian Sea SST and summer insolation during the glacial interval might have been related to the weaker summer monsoon, stronger northeast monsoon, more southerly position of the ITCZ and related feedbacks (Kutzbach and Liu, 1997; Ivanochko et al., 2005; Saraswat et al., 2012).

The Atlantic meridional overturning circulation (AMOC) is another factor that could have influenced heat build-up in the tropical Indian Ocean. A slower AMOC results in reduced transport of warm salty water from the Indian Ocean to the Atlantic Ocean through the Agulhas Current during the glacial period (Beal et al., 2011). The weakening/closure of the Agulhas Current due to the northward migration of the sub-tropical front reduces this cross basin exchange during cold stadials (Bard and Rickaby, 2009). Such reduced cross basin transport would have significantly affect redistribution of heat from the tropical regions to the extratropics. A significant warming during the glacial interval has been noticed in cores collected from the southwestern Indian Ocean part of the Agulhas corridor (Martínez-Méndez et al., 2010). Reduced heat transport from the tropical warm pool, which extends up to the eastern equatorial Indian Ocean, can result in a tremendous increase in seawater temperature in the tropical warm pool (Pierrehumbert, 2000). The tropical Indian Ocean is more vulnerable to such warming due to a readjustment of AMOC, because it is land-locked towards the north, and its northern boundary lies in the tropics, unlike the Pacific Ocean, where dissipation of heat is still possible despite readjusted AMOC, due to possible formation of deepwater along its high latitude northern margin (Okazaki et al., 2010). Regardless of its cause, the early tropical warming in the Indian Ocean might have contributed to the early collapse and retreat of northern ice sheets during deglaciation through the meridional circulation, which is sensitive to tropical perturbations (Cheng et al., 2009; Schmittner and Clement, 2002).

3.4. Deglacial changes in the Indian monsoon and the link to the North Atlantic

The deglacial sequence in the Malabar core reveals a remarkable series of events that reflect the superposition of North Atlantic influences, rapid shifts in the Indian monsoon and the global warming that occurred at the end of the last Ice Age (Fig. 5). This sequence of events begins with an $\delta^{18}O_{sw}$ minimum (i.e., low salinity) at 19.0 (19.1–18.4) kyr, accompanied by a slight maximum in Ba/Ca at 18.8 (18.9–18.3) kyr. The $\delta^{18}O_{sw}$ signal increases steadily by 1.0‰ until 15.9 (16.3–15.0) kyr BP, when it reaches a clear maximum (Figs. 2, 5). This increase runs counter to the small decrease that would be expected from early melting of the ice sheets (Clark et al., 2004) and must reflect a large regional increase in salinity and/or $\delta^{18}O$ of precipitation. The $\delta^{18}O_{sw}$ maximum also coincides with the well-known $\delta^{13}C$ minimum identified in the Malabar core and at other sites, which has been associated with changes in sub-Antarctic circulation (Spero and Lea, 2002).

The slightly elevated Ba/Ca data at 18.8 kyr, 0.87 μmol/mol, indicates some surface runoff and subsequent transport of elevated Ba water from the Bay of Bengal at this time, via the northeast monsoon current (NMC) (Prasanna Kumar et al., 2004). After 18.8 kyr, Ba/Ca drops slightly to a minimum of 0.72 ± 0.03 μmol/mol between 16.7 (17.2–15.8) and 15.1 (15.6 –14.5) kyr BP. (Note that the changes in Ba/Ca are very subtle and close to the error limit.) The very low Ba/Ca in this interval, close to the minimum oceanic value (Lea and Boyle, 1991), indicates that surface waters in the Lakshadweep Sea were characterized by high salinity and were not influenced by transport of high Ba water from the Bay of Bengal via the WMC or by upwelling associated with SMC. Although the very positive $\delta^{18}O_{sw}$ signal supports this interpretation, the larger change, amplified signal and different timing in the $\delta^{18}O_{sw}$ record suggests that this
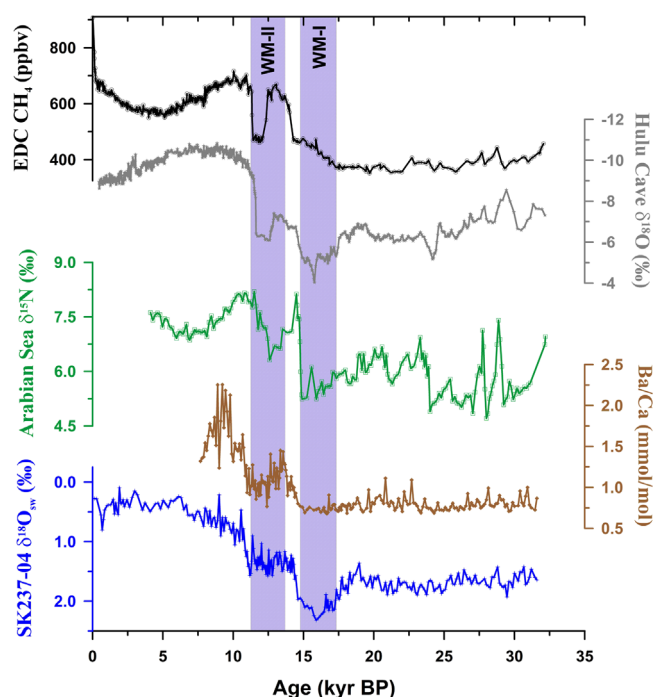
Fig. 5. Comparison of Malabar core $\delta^{18}O$ of seawater and Ba/Ca (surface runoff) records with $\delta^{15}N$ from the eastern Arabian Sea (RC27-14) (Altabet et al., 2002), the Hulu/Dongge Cave $\delta^{18}O$ record from China (Cheng et al., 2009), and the Antarctic (EDC) methane record (Loulerge et al., 2008). The weak monsoon intervals (WMI) inferred from the Hulu Cave record have correlatives in all of the records shown.

proxy was influenced by an additional process. We hypothesize that a regional increase in the $\delta^{18}O$ of precipitation during the weak monsoon interval coinciding with Heinrich Event 1 in the North Atlantic (Pausata et al., 2011) and associated with a southward inter-tropical convergence zone (ITCZ) shift, drove the observed $\delta^{18}O_{sw}$ signal in the Malabar core.

Between 15.9 (16.3–15.0) and 14.3 (15.0–13.8) kyr the $\delta^{18}O_{sw}$ signal drops steadily by 1.0‰, exactly reversing the prior increase (Figs. 2, 5). This trend likely reflects a reversal of the precipitation change described above, as well as the lesser influence of sea level rise, estimated at +0.2‰ in this time interval. The full oscillation in $\delta^{18}O_{sw}$, spanning 19.0 to 14.3 kyr, appears to match similar features in low resolution Pacific records (Lea et al., 2000), suggesting a common tropical phenomenon that might contribute to the observed lag of tropical planktic $\delta^{18}O$ records relative to SST on the deglaciation. During the $\delta^{18}O_{sw}$ recovery, Ba/Ca rises steadily, doubling between 15.1 (15.6–14.5) and 13.6 (14.4–12.6) kyr, with a small maximum at 14.1 (14.6–12.8) kyr. The doubling in Ba/Ca likely reflects enhanced surface runoff and thus transport of low salinity Bay of Bengal water by the NMC, and/or increased riverine Ba input into the Bay of Bengal as the Indian monsoon strengthened following the end of the WMI-1 (i.e., Heinrich 1). Post-glacial, intensification of the Indian monsoon has previously been reported by many workers (Sirocko et al., 1993; Cayre and Bard, 1999; Govil and Naidu, 2010; Banakar et al., 2010). The subsequent shifts in $\delta^{18}O_{sw}$ and Ba/Ca associated with the onset and termination of the YD interval, which are more clearly resolved in the Ba/Ca data, appear to be largely synchronous, as would be expected if both were responding to rainfall and runoff shifts in the Bay of Bengal associated with the onset of the second weak monsoon interval during the YD. After reaching a minimum of < 1 μmol/mol in the YD, Ba/Ca rises rapidly by more than twofold to a maximum > 2 μmol/mol in the early Holocene, 9.8–8.9 (10.7–7.8) kyr BP. The early Holocene maximum likely indicates an enhanced Indian monsoon and associated continental runoff, but

we cannot rule out a diagenetic influence on the highly variable Ba/Ca values in this interval.

Taken as a whole, the interplay between the $\delta^{18}O_{sw}$ and Ba signal between the end of the LGM and the B/A boundary, i.e., the mystery interval (Denton et al., 2006), supports and extends previous inferences of the link between the Indian monsoon and the global monsoon system. Comparison of the two monsoon proxies from the Malabar core with the Hulu Cave record (Sub-tropical China) reveals a strong correspondence (Fig. 5). The LGM $\delta^{18}O$ minimum in the Hulu Cave record is at 19.0 kyr BP, and the post-LGM $\delta^{18}O$ maximum in Hulu is at 16.0 kyr BP (Cheng et al., 2009; Southon et al., 2012), both of which coincide with timing of the correlative $\delta^{18}O_{sw}$ events in the Malabar core. The subsequent $\delta^{18}O$ minimum between 14.5 and 13.8 kyr BP in the Hulu Cave record agrees well with the Malabar $\delta^{18}O_{sw}$ minimum at 14.3 (15.0–13.8) kyr BP. The fact that the timing of the Malabar $\delta^{18}O_{sw}$ record matches the Hulu record so well, as opposed to the less obvious match with the Ba record, supports the interpretation that the Malabar $\delta^{18}O_{sw}$ record dominantly reflects compositional changes in precipitation driven by changes in the North Atlantic (Gupta et al., 2003; Pausata et al., 2011), whereas the Ba record likely reflects the regional influence of the WMC and runoff to the Bay of Bengal, which apparently responded less directly to events in the North Atlantic.

A final point to note is that the Malabar SST record, which rises steadily between 18.6 and 15.7 kyr BP, appears to be completely decoupled over that time interval from both the North Atlantic-driven changes in precipitation and the more regional Indian monsoon changes (Fig. 3). But between 15.7 and 13.2 kyr BP there is a long plateau in SST (Fig. 3). This SST plateau deviates from the dominant low latitude SST trend, which is mostly rising during this interval (Lea, 2004; Shakun et al., 2012) (Fig. 5). This observation suggests that warming in the Lakshadweep Sea was held back during this time interval by a regional process, either via transport of cool waters from the WMC, a current that slightly cools the region today in the winter, or by enhanced upwelling associated with the SMC (Shankar et al., 2004). Although the present data do not allow us to differentiate between these hypotheses, the large Ba anomaly associated with the time interval of the SST plateau support intensified WMC transport of Ba-rich waters from the Bay of Bengal as the source of the cooling, because upwelling would be expected to only slightly elevate surface water Ba concentration.

What emerges from this analysis is that the time interval between 15.9 and 15.1 kyr clearly reflects a climatological hinge point in the Malabar region. Events before 15.9 kyr dominantly reflected teleconnections to Heinrich Event 1, as evidenced by the strong response in the $\delta^{18}O$ of precipitation (Pausata et al., 2011). Events after 15.1 kyr reflected a coordinated response to alternating strong–weak–strong Indian Monsoon precipitation associated, at least in timing, with the onset of the B/A–YD–pre-Boreal, respectively. The availability of high resolution records of $\delta^{18}O_{sw}$ and Ba/Ca from the Bay of Bengal, which should directly reflect Indian Ocean precipitation, would provide a direct test of this hypothesis.

Both the $\delta^{18}O_{sw}$ and Ba/Ca records indicate a two-step deglaciation in the northern Indian Ocean, thus supporting the similar variation observed in foraminiferal $\delta^{18}O$ record from the northeastern Arabian Sea (Cayre and Bard, 1999), change in organic carbon content in the cores (111KL, 136KL) collected from the northwestern Indian Ocean (Schulz et al., 1998) as well as a $\delta^{15}N$ record (Altabet et al., 2002) (Fig. 5). The beginning of the two step deglacial $\delta^{18}O$ depletion coincides with the increase in atmospheric methane as determined from ice cores (Brook et al., 1996; Loulerge et al., 2008). The mid-transition $\delta^{18}O$ plateau also coincides with the decrease in the atmospheric methane concentration. Additionally the two step change in various monsoon

indicators from the northern Indian Ocean also matches well with the Hulu δ^{18}O monsoon record (Cheng et al., 2009) (Fig. 5).

The change in δ^{18}O$_{sw}$ over the last glacial–interglacial transition —that is, the difference between the average of the LGM (19-23 kyr) and the top 5 cm of the core is 1.35 ± 0.18‰. Removing the average ice-volume contribution of $1.0 \pm 0.1\%$ from the total δ^{18}Osw change over the glacial–interglacial transition (Schrag et al., 2002) leaves 0.35 ± 0.21‰, which can be attributed to local salinity changes (i.e., increase of evaporation relative to precipitation or vice versa). Using a regional slope of 0.26‰ change in δ^{18}O$_{sw}$ per unit change in seawater salinity (Delaygue et al., 2001) suggests a 1.4 ± 0.8 su increase during the LGM in the SE Arabian Sea. A higher LGM salinity in this region is consistent with reduced transport of low salinity water from the Bay of Bengal. Previous work suggested a somewhat larger increase (i.e., ~2-4 su) in the northern Indian Ocean (Govil and Naidu, 2010; Banakar et al., 2010).

4. Conclusion

A centennial scale SST and salinity proxy record spanning the last 32 kyr BP from the south-eastern Arabian Sea improves our understanding of tropical deglacial temperature trends, monsoon changes and their role in global climatic variations during glacial–interglacial transitions. This record indicates that the SE Arabian Sea was 2.7 ± 0.5 °C colder during the LGM, and that SSTs began to rise 18.6 (18.8−18.1) kyr BP, during the last glacial termination. Even though the initial SST rise might have preceded the rise in atmospheric CO_2, it is likely that greenhouse gas forcing exerted the dominant control over deglacial warming. A prominent mid-termination SST plateau occurs between 15.7 (16.2−14.9) and 13.2 (13.9−12.0) kyr BP, which might reflect an intensified winter monsoon current. A strong correspondence between the timing of the Malabar δ^{18}O$_{sw}$ record and the Hulu Cave monsoon record suggests that deglacial δ^{18}O changes in both localities dominantly reflect compositional changes in precipitation, likely driven by changes in the North Atlantic (Pausata et al., 2011). A decoupling of SST and monsoon changes in the tropical regions is inferred from the first-ever foraminiferal Ba/Ca-based riverine runoff record covering the last termination in the tropical northern Indian Ocean. Indian sub-continent runoff only began to rise at 15.1 (15.6−14.5) kyr BP, indicating the intensification of the Indian monsoon, coincident with warming in the northern high latitudes after H1, implying a dominant control of North Atlantic processes on the Indian monsoon.

References

Agnihotri, R., Bhattacharya, S.K., Sarin, M.M., Somayajulu, B.L.K., 2003. Changes in surface productivity and subsurface denitrification during the Holocene: a multiproxy study from the eastern Arabian Sea. Holocene 13, 701–713.

Alley, R.B., Clark, P.U., 1999. The deglaciation of the northern hemisphere: a global perspective. Annu. Rev. Earth Planet. Sci. 27, 149–182.

Altabet, M.A., Higginson, M.J., Murray, D.W., 2002. The effect of millennial-scale changes in Arabian Sea denitrification on atmospheric CO_2. Nature 415, 159–162.

Anand, P., Elderfield, H., Conte, M.H., 2003. Calibration of Mg/Ca thermometry in planktonic foraminifera from a sediment trap time series. Paleoceanography 18, 1050, http://dx.doi.org/10.1029/2002PA000846.

Anand, P., Kroon, D., Singh, A.D., Ganeshram, R.S., Ganssen, G., Elderfield, H., 2008. Coupled sea surface temperature–seawater δ^{18}O reconstructions in the Arabian Sea at the millennial scale for the last 35 ka. Paleoceanography 23, PA4207, http://dx.doi.org/10.1029/2007PA001564.

Banakar, V.K., Mahesh, B.S., Burr, G., Chodankar, A.R., 2010. Climatology of the Eastern Arabian Sea during the last glacial cycle reconstructed from paired measurement of foraminiferal δ^{18}O and Mg/Ca. Quat. Res. 73, 535–540.

Bard, E., Rickaby, R.E.M., 2009. Migration of the subtropical front as a modulator of glacial climate. Nature 460, 380–383.

Beal, L.M., De Ruijter, W.P.M., Biastoch, A., Zahn, R., 2011. SCOR/WCRP/IAPSO Working Group, 2011. On the role of the Agulhas system in ocean circulation and climate. Nature 472, 429–436.

Bemis, B.E., Spero, H.J., Bijma, J., Lea, D.W., 1998. Reevaluation of the oxygen isotopic composition of planktonic foraminifera: experimental results and revised paleotemperature equations. Paleoceanography 13, 150–160.

Blaauw, M., Christen, J.A., 2011. Flexible paleoclimate age-depth models using an autoregressive gamma process. Bayesian Anal. 6, 457–474.

Broccoli, A.J., Dahl, K.A., Stouffer, R.J., 2006. Response of the ITCZ to Northern Hemisphere cooling. Geophys. Res. Lett. 33, L01702, http://dx.doi.org/10.1029/ 2005GL024546.

Brook, E.J., Sowers, T., Orchardo, J., 1996. Rapid variations in atmospheric methane concentration during the past 110,000 years. Science 273, 1087–1091.

Cayre, O., Bard, E., 1999. Planktonic foraminiferal and alkenone records of the last deglaciation from the Eastern Arabian Sea. Quat. Res. 52, 337–342.

Chatterjee, P., Goswami, B.N., 2004. Structure, genesis and scale selection of the tropical quasi-biweekly mode. Q. J. R. Meteorol. Soc. 130, 1171–1194.

Cheng, H., Edwards, R.L., Broecker, W.S., Denton, G.H., Kong, X., Wang, Y., Zhang, R., Wang, X., 2009. Ice age terminations. Science 326, 248–252.

Chiang, J.C.H., 2009. The tropics in paleoclimate. Annu. Rev. Earth Planet. Sci. 37, 263–297.

Chiang, J.C.H., Biasutti, M., Battisti, D.S., 2003. Sensitivity of the Atlantic Inter-tropical Convergence Zone to Last Glacial Maximum boundary conditions. Paleoceanography 18, 1094, http://dx.doi.org/10.1029/2003PA000916.

Chodankar, A.R., Banakar, V.K., Oba, T., 2005. Past 100 ky surface salinity gradient response in the Eastern Arabian Sea to the summer monsoon variation recorded by δ^{18}O of G. sacculifer. Glob. Planet. Change 47, 135–142.

Clark, P.U., McCabe, A.M., Mix, A.C., Weaver, A.J., 2004. Rapid rise of sea level 19,000 years ago and its global implications. Science 304, 1141–1144.

Dahl, K.A., Oppo, D.W., 2006. Sea surface temperature pattern reconstructions in the Arabian Sea. Paleoceanography 21, PA1014, http://dx.doi.org/10.1029/ 2005PA001162.

Dekens, P.S., Lea, D.W., Pak, D.K., Spero, H.J., 2002. Core top calibration of Mg/Ca in tropical foraminifera: refining paleotemperature estimation. Geochem. Geo-phys. Geosyst. 3, http://dx.doi.org/10.1029/2001GC000200.

Delaygue, G., Bard, E., Rollion, C., Jouzel, J., Stiévenard, M., Duplessy, J.C., Ganssen, G., 2001. Oxygen isotope/salinity relationship in the northern Indian Ocean. J. Geophys. Res. 106, 4565–4574.

Denton, G., Broecker, W.S., Alley, R.B., 2006. The mystery interval 17.5–14.5 kyrs ago. PAGES News 2, 14–16.

Denton, G.H., Anderson, R.F., Toggweiler, J.R., Edwards, R.L., Schaefer, J.M., Putnam, A.E., 2010. The Last Glacial Termination. Science 328, 1652–1656.

Ding, Q., Steig, E.J., Battisti, D.S., Küttel, M., 2011. Winter warming in West Antarctica caused by central tropical Pacific warming. Nat. Geosci., http://dx. doi.org/10.1038/NGEO1129.

Duplessy, J.C., 1982. Glacial to interglacial contrasts in the northern Indian Ocean. Nature 295, 494–498.

Feldberg, M.J., Mix, A.C., 2003. Planktonic foraminifera, sea surface temperatures, and mechanisms of oceanic change in the Peru and south equatorial currents, 0–150 ka BP. Paleoceanography 18, 1016, http://dx.doi.org/10.1029/2001PA000740.

Gagan, M.K., Ayliffe, L., Drysdale, R., Zhao, J., Griffiths, M.L., Hellstrom, J., Dunbar, G., Hantoro, W., Edwards, R., Cheng, H., Suwargadi, B., 2011. Orbital- and millennial-scale changes in the Australasian monsoon over the last 470,000 years. American Geophysical Union, Fall Meeting 2011, abstract #PP11C-01.

Govil, P., Naidu, P.D., 2010. Evaporation–precipitation changes in the eastern Arabian Sea for the last 68 ka: implications on monsoon variability. Paleocea-nography 25, PA1210, http://dx.doi.org/10.1029/2008PA001687.

Gupta, A.K., Anderson, D.M., Overpeck, J.T., 2003. Abrupt changes in the Holocene Asian southwest monsoon and their links to the North Atlantic Ocean. Nature 421, 354–357.

Hall, J.M., Chan, L.-H., 2004. Ba/Ca in Neogloboquadrina pachyderma as an indicator of deglacial meltwater discharge into the western Arctic Ocean. Paleoceano-graphy 19, PA1017, http://dx.doi.org/10.1029/2003PA000910.

Hönisch, B., Allen, K.A., Russell, A.D., Eggins, S.M., Bijma, J., Spero, H.J., Lea, D.W., Yu, J., 2011. Planktic foraminifers as recorders of seawater Ba/Ca. Mar. Micropaleontol. 79, 52–57.

Ivanochko, T.S., Ganeshram, R.S., Brummer, G.-J.A., Ganssen, G., Jung, S.J.A., Moreton, S.G., Kroon, D., 2005. Variations in tropical convection as an amplifier of global climate change at the millennial scale. Earth Planet. Sci. Lett. 235, 302–314.

Jouzel, J., Masson-Delmotte, V., Cattani, O., Dreyfus, G., Falourd, S., Hoffmann, G., Minster, B., Nouet, J., Barnola, J.-M., Chappellaz, J.A., Fischer, H., Gallet, J.C., Johnsen, S.J., Leuenberger, M., Loulergue, L., Luethi, D., Oerter, H., Parrenin, F., Raisbeck, G., Raynaud, D., Schilt, A., Schwander, J., Selmo, E., Souchez, R., Spahni, R., Stauffer, B., Steffensen, J.P., Stenni, B., Stocker, T.F., Tison, J.-L., Werner, M., Wolff, E.W., 2007. Orbital and millennial Antarctic climate variability over the past 800,000 years. Science 317, 793–797.

Köhler, P., Bintanja, R., Fischer, H., Joos, F., Knutti, R., Lohmann, G., Masson- Delmotte, V., 2010. What caused earth's temperature variations during the last 800,000 years? Data-based evidence on radiative forcing and constraints on climate sensitivity. Quat. Sci. Rev. 29, 129–145.

Krishnamurti, T.N., Bhalme, H.N., 1976. Oscillations of a monsoon system, Part I: observational aspects. J. Atmos. Sci. 33, 1937–1954.

Kutzbach, J.E., Liu, Z., 1997. Feedbacks in the Middle Holocene. Science 278 440–443

Laskar, J., Robutel, P., Joutel, F., Gastineau, M., Correia, A.C.M., Levrard, B., 2004. A long term numerical solution for the insolation quantities of the Earth. Astron. Astrophys. 428, 261–285.

Lea, D.W., Boyle, E.A., 1991. Barium in planktonic foraminifera. Geochim. Cosmochim. Acta 55, 3321–3331.

Lea, D.W., 2004. The 100,000-yr cycle in tropical SST, greenhouse forcing, and climate sensitivity. J. Clim. 17, 2170–2179.

Lea, D.W., Spero, H.J., 1992. Experimental determination of barium uptake in shells of the planktonic foraminifera Orbulina universa at 22 °C. Geochim. Cosmochim. Acta 56, 2673–2680.

Lea, D.W., Spero, H.J., 1994. Assessing the reliability of paleochemical tracers: barium uptake in the shells of planktonic foraminifera. Paleoceanography 9, 445–452.

Lea, D.W., Pak, D.K., Spero, H.J., 2000. Climate impact of late quaternary equatorial pacific sea surface temperature variations. Science 289, 1719–1724.

Lea, D.W., Pak, D.K., Peterson, L.C., Hughen, K.A., 2003. Synchroneity of tropical and high-latitude Atlantic temperatures over the last glacial termination. Science 301, 1361–1364.

Locarnini, R.A., Mishonov, A.V., Antonov, J.I., Boyer, T.P., Garcia, H.E., 2006. World Ocean Atlas 2005, Vol. 1: Temperature. In: Levitus, S. (Ed.), NOAA Atlas NESDIS 61. US Government Printing Office, Washington, DC, 182 pp.

Loulergue, L., Schilt, A., Spahni, R., Masson-Delmotte, V., Blunier, T., Lemieux, B., Barnola, J.-M., Raynauld, D., Stocker, T.F., Chappellaz, J., 2008. Orbital and millennial-scale features of atmospheric CH_4 over the past 800,000 years. Nature 453, 383–386.

Lourantou, A., Lavrič, J.V., Köhler, P., Barnola, J.-M., Paillard, D., Michel, E., Raynaud, D., Chappellaz, J., 2010. Constraint of the CO_2 rise by new atmospheric carbon isotopic measurements during the last deglaciation. Global Biogeochem. Cycles 24, GB2015, http://dx.doi.org/10.1029/2009GB003545.

MARGO Project Members, 2009. Constraints on the magnitude and patterns of ocean cooling at the Last Glacial Maximum. Nat. Geosci. 2, 127–132.

Martin, P.A., Lea, D.W., 2002. A simple evaluation of cleaning procedures on fossil benthic foraminiferal Mg/Ca. Geochem. Geophys. Geosyst., 3, http://dx.doi.org/10.1029/2001GC000280.

Martínez-Méndez, G., Zahn, R., Hall, I.R., Peeters, F.J.C., Pena, L.D., Cacho, I., Negre, C., 2010. Contrasting multiproxy reconstructions of surface ocean hydrography in the Agulhas Corridor and implications for the Agulhas Leakage during the last 345,000 years. Paleoceanography 25, PA4227, http://dx.doi.org/10.1029/2009PA001879.

McCreary Jr., J.P., Kundu, P.K., 1989. A numerical investigation of sea surface temperature variability in the Arabian Sea. J. Geophys. Res. 94, 16097–16114.

McCreary Jr., J.P., Kundu, P.K., Molinari, R.L., 1993. A numerical investigation of dynamics, thermodynamics and mixed-layer processes in the Indian Ocean. Prog. Oceanogr. 31, 181–244.

Monnin, E., Indermuhle, A., Dallenbach, A., Fluckiger, J., Stauffer, B., Stocker, T.F., Raynaud, D., Barnola, J.-M., 2001. Atmospheric CO_2 concentrations over the last glacial termination. Science 291, 112–114.

Murtugudde, R., Busalacchi, A.J., 1999. Interannual variability of the dynamics and thermodynamics of the Indian Ocean. J. Clim. 12, 2300–2326.

Naidu, P.D., Malmgren, B.A., 1996. A high-resolution record of late Quaternary upwelling along the Oman Margin, Arabian Sea based on planktonic foraminifera. Paleoceanography 11, 129–140.

Neema, C.P., Hareeshkumar, P.V., Babu, C.A., 2011. Characteristics of Arabian Sea mini warm pool and Indian summer monsoon. Clim. Dyn. 38 2073–2087

North Greenland Ice Core Project members, 2004. High-resolution record of Northern Hemisphere climate extending into the last interglacial period. Nature 431, 147–151.

Nyadjro, E.S., Subrahmanyam, B., Murty, V.S.N., Shriver, J.F., 2012. The role of salinity on the dynamics of the Arabian Sea mini warm pool. J. Geophys. Res. 117, C09002, http://dx.doi.org/10.1029/2012JC007978.

Okazaki, Y., Timmermann, A., Menviel, L., Harada, N., Abe-Ouchi, A., Chikamoto, M. O., Mouchet, A., Asahi, H., 2010. Deepwater formation in the North Pacific During the Last Glacial termination. Science 329, 200–204.

Parrenin, F., Masson-Delmotte, V., Köhler, P., Raynaud, D., Paillard, D., Schwander, J., Barbante, C., Landais, A., Wegner, A., Jouzel, J., 2013. Synchronous change of atmospheric CO_2 and Antarctic temperature during the last deglacial warming. Science 339, 1060–1063.

Pausata, F.S.R., Battisti, D.S., Nisancioglu, K.H., Bitz, C.M., 2011. Chinese stalagmite $\delta^{18}O$ controlled by changes in the Indian monsoon during a simulated Heinrich event. Nat. Geosci. 4, 474–480.

Pierrehumbert, R.T., 2000. Climate change in the tropical Pacific: the sleeping dragon wakes. Proc. Natl. Acad. Sci. 97, 1355–1358.

Prasanna Kumar, S., et al., 2004. Intrusion of the Bay of Bengal water into the Arabian Sea during winter monsoon and associated chemical and biological response. Geophys. Res. Lett. 31, L15304.

Prell, W.L., Kutzbach, J.E., 1987. Monsoon variability over the past 150,000 years. J. Geophys. Res. 92, 8411–8425.

Prell, W.L., 1984. Variation of monsoonal upwelling a response to changing solar radiation. In: Hansen, J.E., Takahashi, T. (Eds.), Climate Processes and Climate Sensitivity, Geophysical Monograph Series, 19. AGU, Washington, DC, pp. 48–57.

Rao, R.R., Sivakumar, R., 1999. On the possible mechanisms of the evolution of a mini-warm pool during the pre-summer monsoon season and the onset vortex in the southeastern Arabian Sea. Q. J. R. Meteorol. Soc. 125, 787–809.

Rashid, H., England, E., Thompson, L., Polyak, L., 2011. Late glacial to Holocene Indian summer monsoon variability based upon sediment records taken from the Bay of Bengal. Terr. Atmos. Oceanic. 22, 215–228.

Reimer, P.J., Baillie, M.G.L., Bard, E., Bayliss, A., Beck, J.W., Blackwell, P.G., Ramsey, C. B., Buck, C.E., Burr, G.S., Edwards, R.L., Friedrich, M., Grootes, P.M., Guilderson, T. P., Hajdas, I., Heaton, T.J., Hogg, A.G., Hughen, K.A., Kaiser, K.F., Kromer, B., McCormac, F.G., Manning, S.W., Reimer, R.W., Richards, D.A., Southon, J.R., Talamo, S., Turney, C.S.M., van der Plicht, J., Weyhenmeyer, C.E., 2009. Intcal09 and Marine09 radiocarbon age calibration curves, 0–50,000 years cal BP. Radiocarbon 51, 1111–1150.

Rodgers, K.B., Lohmann, G., Lorenz, S., Schneider, R., Henderson, G.M., 2003. A tropical mechanism for Northern Hemisphere deglaciation. Geochem. Geophys. Geosyst. 4, 1046, http://dx.doi.org/10.1029/2003GC000508.

Rostek, F., Ruhland, G., Bassinot, F.C., Muller, P.J., Labeyrie, L.D., Lancelot, Y., Bard, E., 1993. Reconstructing sea surface temperature and salinity using $\delta^{18}O$ and alkenone records. Nature 364, 319–321.

Saher, M.H., Jung, S.J.A., Elderfield, H., Greaves, M.J, Kroon, D., 2007a. Sea surface temperatures of the western Arabian Sea during the last deglaciation. Paleoceanography 22, PA2208, http://dx.doi.org/10.1029/2006PA001292.

Saher, M.H., Peeters, F.J.C., Kroon, D., 2007b. Sea surface temperatures during the SW and NE monsoon seasons in the western Arabian Sea over the past 20,000 years. Palaeogeogr. Palaeoclimatol. Palaeoecol. 249, 216–228.

Saher, M.H., Rostek, F., Jung, S.J.A., Bard, E., Schneider, R.R., Greaves, M., Ganssen, G. M., Elderfield, H., Kroon, D., 2009. Western Arabian Sea SST during the penultimate interglacial: a comparison of U37K′ and Mg/Ca paleothermometry. Paleoceanography 24, PA2212, http://dx.doi.org/10.1029/2007PA001557.

Saraswat, R., Nigam, R., Weldeab, S., Mackensen, A., Naidu, P.D., 2005. A first look at past sea surface temperatures in the equatorial Indian Ocean from Mg/Ca in foraminifera. Geophys. Res. Lett. 32, L24605, http://dx.doi.org/10.1029/2005GL024093.

Saraswat, R., Nigam, R., Weldeab, S., Mackensen, A., 2007. The tropical warm pool in the Indian Ocean and its influence on ENSO over the past 137,000 yrs BP. Curr. Sci. 92, 1153–1156.

Saraswat, R., Nigam, R., Mackensen, A., Weldeab, S., 2012. Linkage between seasonal insolation gradient in the tropical northern hemisphere and the sea surface salinity of the equatorial Indian Ocean during the last glacial period. Acta Geol. Sin. 86, 801–811.

Sarkar, A., Ramesh, R., Bhattacharya, S.K., Rajagopalan, G., 1990. Oxygen isotope evidence for a stronger winter monsoon current during the last glaciation. Nature 343, 549–551.

Sarnthein, M., Grootes, P.M., Holbourn, A., Kuhnt, W., Kühn, H., 2011. Tropical warming in the Timor Sea led deglacial Antarctic warming and atmospheric CO_2 rise by more than 500 yr. Earth Planet. Sci. Lett. 302, 337–348.

Schmidt, M.W., Lynch-Stieglitz, J., 2011. Florida Straits deglacial temperature and salinity change: implications for tropical hydrologic cycle variability during the Younger Dryas. Paleoceanography 26, PA4205, http://dx.doi.org/10.1029/2011PA002157.

Schmitt, J., Schneider, R., Elsig, J., Leuenberger, D., Lourantou, A., Chappellaz, J., Köhler, P., Joos, F., Stocker, T.F., Leuenberger, M., Fischer, H., 2012. Carbon isotope constraints on the deglacial CO_2 rise from ice cores. Science 336, 711–714.

Schmittner, A., Clement, A.C., 2002. Sensitivity of the thermohaline circulation to tropical and high latitude freshwater forcing during the last glacial–interglacial cycle. Paleoceanography 17, 1017, http://dx.doi.org/10.1029/2000PA000591.

Schrag, D.P., Adkins, J.F., McIntyre, K., Alexander, J.L., Hodell, D.A., Charles, C.D., McManus, J.F., 2002. The oxygen isotopic composition of seawater during the Last Glacial Maximum. Quat. Sci. Rev. 21, 331–342.

Schulz, H., Rad, U., Erlenkeuser, H., 1998. Correlation between Arabian Sea and Greenland climate oscillations of the past 110,000 years. Nature 393, 54–57.

Sengupta, D., Ray, P.K., Bhat, G.S., 2002. Spring warming of the eastern Arabian Sea and Bay of Bengal from buoy data. Geophys. Res. Lett. 29, 1734, http://dx.doi.org/10.1029/2002GL015340.

Sengupta, D., Parampil, S.R., Bhat, G.S., Murty, V.S.N., Ramesh Babu, V., Sudhakar, T., Premkumar, K., Pradhan, Y., 2008. Warm pool thermodynamics from the Arabian Sea Monsoon Experiment (ARMEX). J. Geophys. Res. 113, C10008, http://dx.doi.org/10.1029/2007JC004623.

Shakun, J.D., Clark, P.U., He, F., Marcott, S.A., Mix, A.C., Liu, Z., Otto-Bliesner, B., Schmittner, A., Bard, E., 2012. Global warming preceded by increasing carbon dioxide concentrations during the last deglaciation. Nature 484, 49–54.

Shankar, D., Gopalakrishna, V.V., Shenoi, S.S.C., Durand, F., Shetye, S.R., Rajan, C.K., Johnson, Z., Araligidad, N., Michael, G.S., 2004. Observational evidence for

westward propagation of temperature inversions in the southeastern Arabian Sea. Geophys. Res. Lett. 31, L08305, http://dx.doi.org/10.1029/2004GL019652.

Shankar, D., Vinaychandran, P.N., Unnikrishnan, A.S., 2002. The monsoon currents in the north Indian Ocean. Prog. Oceanogr. 52, 63–120.

Shenoi, S.S.C., Shankar, D., Shetye, S.R., 1999. The sea surface temperature high in the Lakshadweep Sea before the onset of the southwest monsoon. J. Geophys. Res. 104, 703–712.

Shenoi, S.S.C., Shankar, D., Gopalakrishna, V.V., Durand, F., 2005. Role of ocean in the genesis and annihilation of the core of the warm pool in the southeastern Arabian Sea. Mausam 56, 147–161.

Sirocko, F., Sarnthein, M., Erlenkeuser, H., Lange, H., Arnold, M., Duplessy, J.-C., 1993. Century-scale events in monsoonal climate over the past 24,000 years. Nature 364, 322–324.

Southon, J., Kashgarian, M., Fontugne, M., Metivier, B., Yim, W.W.-S., 2002. Marine reservoir corrections for the Indian Ocean and Southeast Asia. Radiocarbon 44, 167–180.

Southon, J., Noronha, A.L., Cheng, H., Edwards, R.L., Wang, Y., 2012. A high-resolution record of atmospheric ^{14}C based on Hulu Cave speleothem H82. Quat. Sci. Rev. 33, 32–41.

Spero, H.J., Lea, D.W., 2002. The cause of carbon isotope minimum events on glacial terminations. Science 296, 522–525.

Stuiver, M., Reimer, P.J., 1993. Extended ^{14}C database and revised CALIB radiocarbon calibration program. Radiocarbon 35, 215–230.

Swallow, J., 1984. Some aspects of the physical oceanography of the Indian Ocean. Deep-Sea Res. Part A Oceanogr. Res. 31, 639–650.

Tiwari, M., Ramesh, R., Somayajulu, B.L.K., Jull, A.J.T., Burr, G.S., 2005. Early deglacial (19–17 ka) strengthening of the northeast monsoon. Geophys. Res. Lett. 32, L19712, http://dx.doi.org/10.1029/2005GL024070.

Trenberth, K.E., Fasullo, J.T., O'Dell, C., Wong, T., 2010. Relationships between tropical sea surface temperature and top of atmosphere radiation. Geophys. Res. Lett. 37, L03702, http://dx.doi.org/10.1029/2009GL042314.

Vinayachandran, P.N., Shetye, S.R., 1991. The warm pool in the Indian Ocean. Proc. Indian Acad. Sci. (Earth Planet. Sci.) 100, 165–175.

Weldeab, S., Lea, D.W., Schneider, R.R., Andersen, N., 2007. 155,000 years of West African monsoon and ocean thermal evolution. Science 316, 1303–1307.

Yuan, X.J., Martinson, D.G., 2000. Antarctic sea ice extent variability and its global connectivity. J. Clim. 13, 1697–1717.